Progress In Electromagnetics Research, PIER 95, 267–282, 2009

SENSOR SELECTION FOR TARGET TRACKING IN SENSOR NETWORKS

H. Q. Liu, H. C. So, K. W. K. Lui, and F. K. W. Chan

Department of Electronic Engineering
City University of Hong Kong
Tat Chee Avenue, Kowloon, Hong Kong, China

Abstract—This paper addresses the sensor selection problem which is a very important issue where many sensors are available to track a target. In this problem, we need to select an appropriate group of sensors at each time to perform tracking in a wireless sensor network (WSN). As the theoretical tracking performance is bounded by posterior Cramer-Rao lower bound (PCRLB), it is used as a criterion to select sensors. Based on the PCRLB, sensor selection algorithms with and without sensing range constraint are developed. Without sensing range limit, exhaustive enumeration is first adopted to search all possible combinations for sensor selection. To reduce complexity of enumeration, second, we restrict the selected sensors to be within a fixed area in the WSN. With sensing range constraint, a circle will be drawn with the help of communication range for sensor selection. In a similar manner, two approaches, namely, selecting all sensors inside the circle or using enumeration to select sensors within the circle are presented. The effectiveness of the proposed methods is validated by computer simulation results in target tracking for WSNs.

1. INTRODUCTION

The research topic of wireless sensor network (WSN) has attracted much attention over the past few years. The WSNs have wide applications in environmental, medical, food-safety and habitat monitoring, assessing the health of machines, aerospace vehicles and civil engineering structures, energy management, inventory control, home and building automation, homeland security and military initiatives [1, 2]. In this work, we investigate the target tracking problem in a huge WSN where a large number of sensors are available

Corresponding author: H. Q. Liu (hongqiliu2@student.cityu.edu.hk).

for taking measurements. Obviously, the tracking accuracy of a target improves with the increasing number of measurements. Therefore, in terms of the tracking performance, it is desirable to use as many measurements as possible. However, the nodes in the WSNs have limitations in energy consumption, computation power and sensing ranges, which means that it is inappropriate for all available sensors to take measurements. As a result, selecting only a proper group of sensors from the available set to perform tracking is of research value [3–7].

Based on information principles, sensor selection methods are proposed in [3, 4]. In their approaches, at each time only one sensor, referred to as the leader node, is activated. By considering a generic sensor model where the measurements are interpreted as polygonal convex subsets of the plane, [5] proposes a sensor selection method to estimate position of a target with cameras. In [6], using convex optimization followed by a greedy local search, sensor selection problem is solved for multiple target tracking. Employing the expected mean square state estimation error to choose sensors is presented in [7]. According to different channel conditions, the optimization problem for sensors with lower signal-to-noise ratios (SNRs) allocating a larger fraction of the total power is developed in [8].

In this paper, we utilize the posterior Cramér-Rao lower bound (PCRLB) and particle filter (PF) for the joint sensor selection and target tracking problem, since PF has found a lot of successful applications in the area of target tracking [9, 16]. Actually, our procedure includes two major steps: in the first step a number of sensors are selected to provide observations, in the second step, after receiving observations, target tracking is performed by PFs. The performance of tracking system based on Bayesian framework is measured by PCRLB. As a result, PCRLB is a standard and reasonable choice for sensor selection. We consider two interesting scenarios of received measurements: without and with sensing range constraint. First, without sensing range constraint, which means that all sensors are available to take measurements, a combinatorial optimization problem is formulated based on PCRLB. Enumeration search is then performed to determine the combination of sensors to seek for the minimum value of PCRLB. Here, PCRLB does not evaluate the expectation of joint probability density function (PDF) of states and measurements as we assume that process noise is zero [9]. Even when the process noise is present, as confirmed by simulations, the tracking system does not suffer from much performance loss, and this phenomenon is also pointed out in [9]. The enumeration search would be a huge computational burden even when the density of a sensor network is just medium. In order to reduce complexity, we propose to restrict a fixed area such as square or rectangle in the search. The sensors within the area that gives minimum PCRLB value will be selected to perform tracking. Second, we consider the case with sensing range constraint, which means that not all sensors can take measurements. However, the sensor communication range will be utilized. According to the predicted position of the target a circle would be drawn, and then the sensors inside the circle are chosen to perform sensing task. This approach is a generalization of nearest neighborhood (NN) method [4], which selects only one sensor closest to the predicted position. Instead of using all sensors within the circle, an alternative is that enumeration search technique is used again to select sensors based on PCRLB. Since the successful applications [11–13] of PFs in nonlinear and/or non-Gaussian models, they are adopted in the nonlinear target tracking problem. To improve the PF performance, assigning extended Kalman filter (EKF) [9] and unscented Kalman filter (UKF) [10] as importance sampling functions are also suggested. The main contribution of the paper is that four different search strategies are developed to select sensors in target tracking based on PCRLB.

The rest of the paper is organized as follows. The problem formulation of target tracking with sensor selection is presented in Section 2. A brief introduction of PF is given in Section 3. In Section 4, sensor selection approaches are presented to perform tracking using PFs. In Section 5, simulation results for evaluating the tracking performance of the proposed algorithms are provided. Finally, conclusions are drawn in Section 6.

2. PROBLEM FORMULATION

The model-based methods for tracking applications requires at least two models: the state model which describes the evolution of the state with time, and the measurement model which defines the relationship between noisy observations and the state. In case of two-dimensional (2D) target tracking, let $\mathbf{x}_t = [x_t, y_t, \dot{x}_t, \dot{y}_t]^T$ be state vector that represents the coordinates and velocities of a moving target at time t. In this paper, linear state and nonlinear measurement models are considered [4, 12]:

$$\mathbf{x}_t = f(\mathbf{x}_{t-1}) + \mathbf{v}_t = \mathbf{F}\mathbf{x}_{t-1} + \mathbf{v}_t \tag{1}$$

and

$$\mathbf{z}_t = g(\mathbf{x}_t) + \mathbf{w}_t \tag{2}$$

where

$$\mathbf{F} = \begin{bmatrix} 1 & 0 & T_s & 0 \\ 0 & 1 & 0 & T_s \\ 0 & 0 & 1 & 0 \\ 0 & 0 & 0 & 1 \end{bmatrix}$$

The T_s is the sampling interval, $\mathbf{v}_t$ is a 4×1 independent and identically distributed process noise vector with $\mathbf{v}_t \sim \mathcal{N}(\mathbf{0}, \mathbf{Q})$, $\mathbf{0}$ is a zero vector and $\mathbf{Q} = \mathbf{D}\text{diag}\{\sigma_x^2, \sigma_y^2\}\mathbf{D}^T$, where σ_x^2 and σ_y^2 account the variances in x-coordinate and y-coordinate, and $\mathbf{D}$ has the form of

$$\mathbf{D} = \begin{bmatrix} T_s^2/2 & 0 \\ 0 & T_s^2/2 \\ T_s & 0 \\ 0 & T_s \end{bmatrix}$$

For the measurement model, time-of-arrival (TOA) measurements are used, of course, other typical observations, such as time-difference-of-arrival, angle-of-arrival, received-signal-strength are straightforward to use. By multiplying the TOAs with the known propagation speed, the observed distance measurement at time t of the jth sensor is:

$$\begin{aligned} z_{t,j} = d_{t,j} + w_{t,j} = \sqrt{(x_t - x_j)^2 + (y_t - y_j)^2} + w_{t,j}, \\ t = 1, 2, \ldots, j \in \Phi_t, \quad |\Phi_t| = M_t, \quad \Phi_t \subseteq \{1, 2, \ldots, M\} \end{aligned} \tag{3}$$

where M is the total number of sensors in the WSN, $|\cdot|$ represents cardinality number, x_j and y_j denote the coordinates of jth sensor, $\mathbf{w}_t$ is a zero-mean white Gaussian noise vector containing $\{w_{t,j}\} \sim \mathcal{N}(0, \sigma_{t,j}^2)$ with length of M_t. The noise covariance matrix is denoted by $\mathbf{R}_t = \text{diag}\{\sigma_{t,1}^2, \ldots, \sigma_{t,j}^2\}$. The M_t represents the number of sensors being selected to provide observations at time t, where it is unknown and may change over time. In this paper, all data are collected in a central unit, therefore, the major objective of our work is to properly determine M_t sensors for tracking in a centralized way.

3. PARTICLE FILTER

In order to track a target under Bayesian framework, we need to calculate the posterior PDF of the state, i.e., $\pi(\mathbf{x}_t|\mathbf{z}_{1:t})$, where $\mathbf{z}_{1:t} = \{\mathbf{z}_1, \mathbf{z}_2, \cdots, \mathbf{z}_t\}$ denotes all the observations up to the current time t. Let the initial density of the state vector be $\pi(\mathbf{x}_0) = \pi(\mathbf{x}_0|\mathbf{z}_0)$, where $\mathbf{z}_0$ means no measurements. The PDF $\pi(\mathbf{x}_t|\mathbf{z}_{1:t})$ is obtained recursively in two stages, namely, prediction and update. Assuming that at time

$(t-1)$ the required PDF $\pi(\mathbf{x}_{t-1}|\mathbf{z}_{1:t-1})$ is available, the prediction density of the state at time t is obtained by the following equation

$$\pi(\mathbf{x}_t|\mathbf{z}_{1:t-1}) = \int p\,(\mathbf{x}_t|\mathbf{x}_{t-1})\pi(\mathbf{x}_{t-1}|\mathbf{z}_{1:t-1})\,d\mathbf{x}_{t-1} \tag{4}$$

At time t the observation $\mathbf{z}_t$ becomes available, the update stage is performed. Via the Bayes' rule, an update of the prediction density is given as

$$\pi(\mathbf{x}_t|\mathbf{z}_{1:t}) \propto p(\mathbf{z}_t|\mathbf{x}_t)\pi(\mathbf{x}_t|\mathbf{z}_{1:t-1}) \tag{5}$$

The recursive propagation of the posterior density, using (4) and (5), is only a conceptual solution in the sense that in general it cannot be determined analytically. The most successful methodology for (4) and (5) is called sequential Monte Carlo method [9, 11], also known as PF, which is an efficient way to solve nonlinear and/or non-Gaussian problems. The key idea behind PF is to represent the required posterior density function by a set of random samples with associated weights and to compute estimates based on these samples and weights. According to the law of large numbers, this Monte Carlo method becomes an equivalent representation of the usual functional description, and the sequential importance sampling approaches the optimal Bayesian estimator. Given the large set of N particles $\{\mathbf{x}_{t-1}^{(i)}\}_{i=1}^{N}$ and their associated weights $\{w_{t-1}^{(i)}\}_{i=1}^{N}$. The posterior density at time $(t-1)$ is approximated as

$$\pi(\mathbf{x}_{t-1}|\mathbf{z}_{1:t-1}) \approx \sum_{i=1}^{N} w_{t-1}^{(i)}\delta\left(\mathbf{x}_{t-1}-\mathbf{x}_{t-1}^{(i)}\right) \tag{6}$$

where $\delta()$ is the Dirac delta function. Moreover, the new particles $\{\mathbf{x}_t^{(i)}\}_{i=1}^{N}$ are generated from the properly designed proposal function:

$$\mathbf{x}_t^{(i)} \sim q\left(\mathbf{x}_t|\mathbf{x}_{t-1}^{(i)},\mathbf{z}_{1:t}\right), \qquad i=1,\ldots,N \tag{7}$$

while the importance weight $w_t^{(i)}$ is recursively updated as

$$w_t^{(i)} \propto w_{t-1}^{(i)} \times \frac{p\left(\mathbf{z}_t|\mathbf{x}_t^{(i)}\right)p\left(\mathbf{x}_t^{(i)}|\mathbf{x}_{t-1}^{(i)}\right)}{q\left(\mathbf{x}_t|\mathbf{x}_{t-1}^{(i)},\mathbf{z}_{1:t}\right)} \tag{8}$$

Based on the new particles and their associated weights, the minimum mean square error (MMSE) estimate is [9]

$$\hat{\mathbf{x}}_t = \mathbb{E}[\mathbf{x}_t|\mathbf{z}_{1:t}] = \int \mathbf{x}_t\pi(\mathbf{x}_t|\mathbf{z}_{1:t})\,d\mathbf{x}_t \approx \sum_{i=1}^{N} w_t^{(i)}\mathbf{x}_t^{(i)} \tag{9}$$

where $\mathbb{E}$ denotes the expectation operator. Since the PF uses the designed proposal function to generate new particles and evaluates their associated importance weights using new observed data, it approximates the posterior PDF well. In PFs after a certain number of recursive steps, all but one particle will have negligible weights, leading to the degeneracy phenomenon. In order to avoid this problem, the resampling step must be taken. Resampling eliminates samples with low importance weights and multiplies samples with high importance weights, and the details can be found in [9]. Another issue in designing a PF is how to choose the proposal functions. In this paper, transition prior, EKF and UKF are adopted as proposal functions. The transition prior uses the transition model in (1) and the details of EKF and UKF are given in [9]. In our algorithm, we assume that a large number of sensors are randomly deployed on the sensor field. Due to the constraints of WSNs, using all sensors at each time to perform tracking is not recommended. The sensor selection problem will be discussed in the next section.

4. SENSOR SELECTION STRATEGIES

4.1. Posterior Cramer-Rao Lower Bound

Let $\hat{\mathbf{x}}_t$ be an unbiased estimate of the state vector $\mathbf{x}_t$, based on $\mathbf{z}_{1:t}$. The covariance matrix of $\mathbf{x}_t$, denoted by $\mathbf{P}_t$, has a lower bound defined as

$$\mathbf{P}_t \triangleq \mathbb{E}\left\{(\hat{\mathbf{x}}_t - \mathbf{x}_t)(\hat{\mathbf{x}}_t - \mathbf{x}_t)^T\right\} \geq \mathbf{J}_t^{-1} \tag{10}$$

where $\mathbf{J}_t^{-1}$ is the PCRLB that bounds the performance of any unbiased estimator. In this paper, PCRLB will be exploited as a criterion to select sensors.

In [14], a recursive method to compute the Fisher information matrix $\mathbf{J}_t$ at time t is derived:

$$\mathbf{J}_{t+1} = \mathbf{D}_t^{22} - \mathbf{D}_t^{21}\left(\mathbf{J}_t + \mathbf{D}_t^{11}\right)^{-1}\mathbf{D}_t^{12} \tag{11}$$

where

$$\begin{aligned}
\mathbf{D}_t^{11} &= -\mathbb{E}\{\nabla_{\mathbf{x}_t}[\nabla_{\mathbf{x}_t} \log p(\mathbf{x}_{t+1}|\mathbf{x}_t)]^T\} \\
\mathbf{D}_t^{21} &= -\mathbb{E}\{\nabla_{\mathbf{x}_t}[\nabla_{\mathbf{x}_{t+1}} \log p(\mathbf{x}_{t+1}|\mathbf{x}_t)]^T\} \\
\mathbf{D}_t^{12} &= [\mathbf{D}_t^{21}]^T \\
\mathbf{D}_t^{22} &= -\mathbb{E}\{\nabla_{\mathbf{x}_{t+1}}[\nabla_{\mathbf{x}_{t+1}} \log p(\mathbf{x}_{t+1}|\mathbf{x}_t)]^T\} \\
&\quad -\mathbb{E}\{\nabla_{\mathbf{x}_{t+1}}[\nabla_{\mathbf{x}_{t+1}} \log p(\mathbf{z}_{t+1}|\mathbf{x}_t)]^T\}
\end{aligned}$$

In case of the additive Gaussian noise, the expressions of $\mathbf{D}_t^{11}$, $\mathbf{D}_t^{12}$ and $\mathbf{D}_t^{22}$ are simplified as follows:

$$\mathbf{D}_t^{11} = \mathbf{F}^T\mathbf{Q}^{-1}\mathbf{F} \tag{12}$$
$$\mathbf{D}_t^{12} = -\mathbf{F}^T\mathbf{Q}^{-1} \tag{13}$$
$$\mathbf{D}_t^{22} = \mathbf{Q}^{-1} + \mathbb{E}\left\{\mathbf{H}_{t+1}^T\mathbf{R}_t^{-1}\mathbf{H}_{t+1}\right\} \tag{14}$$

where $\mathbf{H}_{t+1}$ is the Jacobian of $g(\mathbf{x}_{t+1})$ evaluated at the true value of $\mathbf{x}_{t+1}$, i.e.,

$$\mathbf{H}_{t+1} = [\nabla_{\mathbf{x}_{t+1}} g(\mathbf{x}_{t+1})]^T$$

In our TOA model, $\mathbf{H}_{t+1}$ is

$$\mathbf{H}_{t+1} = \left[\frac{2x_{t+1}}{\sqrt{(x_{t+1}-x_i)^2+(y_{t+1}-y_i)^2}} \frac{2y_{t+1}}{\sqrt{(x_{t+1}-x_i)^2+(y_{t+1}-y_i)^2}} \, 0 \, 0\right]^T \tag{15}$$

Then, the recursion of $\mathbf{J}_t$ can be written as:

$$\mathbf{J}_{t+1}=\mathbf{Q}^{-1}+\mathbb{E}\{\mathbf{H}_{t+1}^T\mathbf{R}_t^{-1}\mathbf{H}_{t+1}\}-\mathbf{Q}^{-1}\mathbf{F}(\mathbf{J}_t+\mathbf{F}^T\mathbf{Q}^{-1}\mathbf{F})^{-1}\mathbf{F}^T\mathbf{Q}^{-1} \tag{16}$$

Assuming that there is no process noise, that is, $\mathbf{Q} = \mathbf{0}$, $\mathbf{J}_{t+1}$ is simplified as:

$$\mathbf{J}_{t+1} = \left[\mathbf{F}^{-1}\right]^T \mathbf{J}_t\mathbf{F}^{-1} + \mathbf{H}_{t+1}^T\mathbf{R}_t^{-1}\mathbf{H}_{t+1} \tag{17}$$

The $\mathbf{J}_t^{-1}$ is PCRLB, which serves as a tool for comparison of implemented filtering method and prediction of the system performance. The diagonal elements of $\mathbf{J}_t^1$ are the lower bounds for the corresponding mean square errors (MSEs). In fact, [9] shows that PCRLB does not have much difference even if the process noise is present. Notice that since the position $[x_{t+1}\ y_{t+1}]^T$ is unavailable at time $(t+1)$, the predicted mean position $[\bar{x}_{t+1}\ \bar{y}_{t+1}]^T$ is used to approximate it, where $\bar{x}_{t+1} = \sum_{i=1}^N w_t^{(i)}\hat{x}_{t+1}^i$, $\bar{y}_{t+1} = \sum_{i=1}^N w_t^{(i)}\hat{y}_{t+1}^i$, where $[\hat{x}_{t+1}^i, \hat{y}_{t+1}^i]$ is the predicted position of ith particle at time $(t+1)$. In doing so, the recursion of $\mathbf{J}_{t+1}$ is also an approximation.

As a useful tool to predict the achievable performance of a tracking system, the PCRLB of (17) is used as a criterion to select sensors to optimize tracking accuracy.

4.2. Approaches without Sensing Range Constraint

Now we assume that all sensor measurements are available. Let $[\mathbf{J}^{-1}]_{i,j}$ be the (i,j) entry of $\mathbf{J}^{-1}$, the corresponding predicted PCRLB for the position is

$$\mathcal{C}_{t+1} = \left[\mathbf{J}_{t+1}^{-1}\right]_{1,1} + \left[\mathbf{J}_{t+1}^{-1}\right]_{2,2} \tag{18}$$

Generally, we want to select M_t sensors to minimize the PCRLB, which leads to the following combinational optimization problem

$$c(M_t)_{opt} \triangleq \arg \min_{c(M_t)\subset\mathcal{L}} \mathcal{C}_{t+1}(c(M_t)) \tag{19}$$

where $c(M_t)$ is the set containing M_t sensors and $\mathcal{L}$ represents the set of all sensors. We need to determine the combination of sensors that minimizes the PCRLB. At first attempt, the number of sensors involved is fixed at each time. Specifically, at each time M_t sensors are chosen to collect information from the target. The built-in command *combnk* in MATLAB is employed to generate combinations. The M_t is a user-chosen parameter. The problem with this search technique is that the complexity will grow exponentially with the total number of sensors, which will be an impossible task to produce all the combinations in larger WSNs. We refer this approach to as Approach 1.

Since the first approach needs to search all combinations in the WSN, to reduce high complexity, we resort to a different selection strategy. Instead of fixing the number of sensors, we fix the area. Specifically speaking, at each time a fixed frame moves on the sensor field, the frame with the minimum PCRLB will be chosen, and then the sensors fall in this area are activated to report target distance information. Note that, in doing so, at every time the number of selected sensors varies with time. Mathematically, it is

$$s(M_t)_{opt} \triangleq \arg \min_{s(M_t)\subset\mathcal{S}} \mathcal{C}_{t+1}(s(M_t)) \tag{20}$$

where $s(M_t)$ denotes the set of sensors in the area s and $\mathcal{S}$ represents the set of whole sensor region. The area could be chosen as a square or a rectangle. It is also a trade-off between the performance and complexity. The bigger area we set, the better performance we can get but more resources are needed. Since this search methodology is based on a chosen area, it is faster than the Approach 1. We refer this to as Approach 2.

4.3. Approaches with Sensing Range Constraint

Sensor sensing range could limit the number of the measurements available. That means we cannot obtain all observations every time. Therefore, we propose the following methods to select sensors with sensing range constraint. Since the predicted mean of position at time $(t+1)$ is available, it would be utilized to select sensors. Using $[\bar{x}_{t+1}\ \ \bar{y}_{t+1}]^T$ as a centre to draw a circle, that sensors lie in this circle will be selected. The radius r of the circle is equal to the maximum sensing range. The sensors are unable to provide measurement information when they are outside the sensing range. In mathematical expression, the sensing range constraint gives

$$(\bar{x}_{t+1} - x_i)^2 + (\bar{y}_{t+1} - y_i)^2 \leq r^2 \tag{21}$$

Since the predicted values provide a rough estimate of target as long as the state model fits to the target movement, the circle will definitely contain the true position of target as well as the number of sensors that are near to the target. In doing so, this approach avoids any complicated computation. Notice that the number of selected sensors at each time also changes with time. We refer this to as Approach 3.

Instead of selecting the all sensors inside the circle, the combination optimization search in (19) could be also accomplished to select a fixed number of M_t sensors, i.e.,

$$c(M_t)_{opt} \triangleq \arg \min_{c(M_t) \subset \mathcal{O}} \mathcal{C}_{t+1}(c(M_t)) \tag{22}$$

where $\mathcal{O}$ represents the set of all sensors in the circle characterized by (21). We refer this to as Approach 4. In summary, the pseudo-code of PF in target tracking with sensor selection is given in Table 1.

5. SIMULATION RESULTS

Computer simulations have been conducted to evaluate the tracking performance of the proposed methods by comparing with selecting one sensor prediction-based NN (1-PNN), three sensors 3-PNN approaches [4] and PCRLB. The MSE is chosen as the performance measure. Particle filtering schemes with transition prior, EKF and UKF as proposal functions are denoted by PF, PF-EKF and PF-UKF, respectively, and we also integrate them in [4]. We assume that M sensors are randomly deployed on a 2D WSN of dimension $500\,\mathrm{m} \times 500\,\mathrm{m}$ and the initial state vector of the target is $[50\,\mathrm{m}, 40\,\mathrm{m}, 7\,\mathrm{m/s}, 6\,\mathrm{m/s}]^T$. The SNR is defined by $\mathrm{SNR} = d_{t,j}^2/\sigma_{t,j}^2$ and is set to be 40 dB. In Approaches 1 and 4, at each time $M_t = 3$ sensors are activated to provide the observations. The number of particles is $N = 500$. The states are initialized randomly around their true values. The Fisher information matrix $\mathbf{J}_0$ is initialized using the identity matrix. Two scenarios of process noise, namely, zero process noise and nonzero process noise of $\sigma_x^2 = \sigma_y^2 = 1$, are investigated. All results provided are averages of 500 independent runs. For each case, we will recommend a tracker based on following rules: If the PF-EKF and PF-UKF have comparable performance, then the PF-EKF will be selected as a tracker as it has less complexity than PF-UKF, otherwise, the PF-UKF will be selected because it has better performance thanks to the usage of UKF as a proposal function.

Table 1. Particle filter with sensor selection.

- Initialization: $t = 0$
  - For $i = 1, \ldots, N$, sample the state particle $\mathbf{x}_0^i \sim p(\mathbf{x}_0)$
- For $t = 1, 2, ...$
  - Sensor selection step:
    - For $i = 1, \ldots, N$, predict the particles according to the sate model
    - Select sensors to provide measurements based on (19), (20), (21) or (22)
  - Importance sampling step:
    - For $i = 1, \ldots, N$, draw particles $\mathbf{x}_t^{(i)} \sim q\left(\mathbf{x}_t|\mathbf{x}_{t-1}^{(i)}, \mathbf{y}_{1:t}\right)$
    - here, three importance sampling functions are available: transition prior, EKF and UKF.
    - For $i = 1, \ldots, N$, evaluate the importance weight: $w_t^{(i)} \propto w_{t-1}^{(i)} \times \frac{p\left(\mathbf{y}_t|\mathbf{x}_t^{(i)}\right)p\left(\mathbf{x}_t^{(i)}|\mathbf{x}_{t-1}^{(i)}\right)}{q\left(\mathbf{x}_t|\mathbf{x}_{t-1}^{(i)},\mathbf{y}_{1:t}\right)}$
    - For $i = 1, \ldots, N$, normalize the importance weight: $\tilde{w}_t^i = w_t^i / \sum_{j=1}^N w_t^j$
  - Resampling step:
    - Eliminate samples with low importance weights and multiply samples with high importance weights.
    - For $i = 1, \ldots, N$, set $w_t^i = 1/N$.
  - MCMC move step:
    - Apply MCMC move to improve the diversity of particles
  - Estimation step:
    - The MMSE estimate of state is obtained as: $\hat{\mathbf{x}}_t \approx \sum_{i=1}^N w_t^{(i)} \mathbf{x}_t^{(i)}$

5.1. Evaluation of Approaches without Sensing Range Constraint

We first study Approach 1 with a total of $M = 40$ sensors. The MSEs of Approach 1 and 1-PNN and 3-PNN technique without and with process noise are plotted in Figures 1 and 2, respectively. We observe that the PF-EKF and PF-UKF of Approach 1 are comparable and they give the best performance using the optimization solution of (19). As PF-UKF requires a higher complexity, the PF-EKF of Approach 1 is recommended as the best tracker in this case. Moreover, it is seen

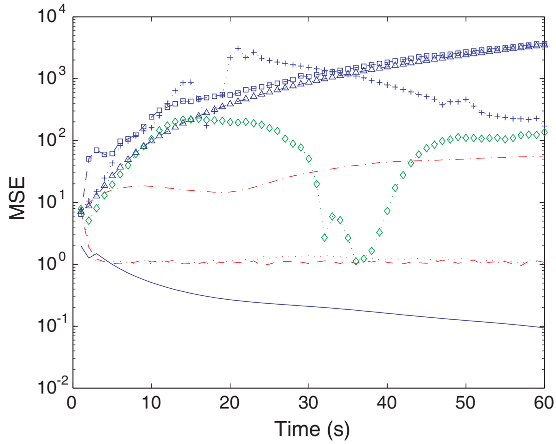

Figure 1. Mean square error comparison between Approach 1, 1-PNN and 3-PNN methods without process noise (— PCRLB; - · - PF of Approach 1; −− PF-EKF of Approach 1; ··· PF-UKF of Approach 1; △ PF of 1-PNN; □ PF-EKF of 1-PNN; + PF-UKF of 1-PNN; ⋄ PF-UKF of 3-PNN).

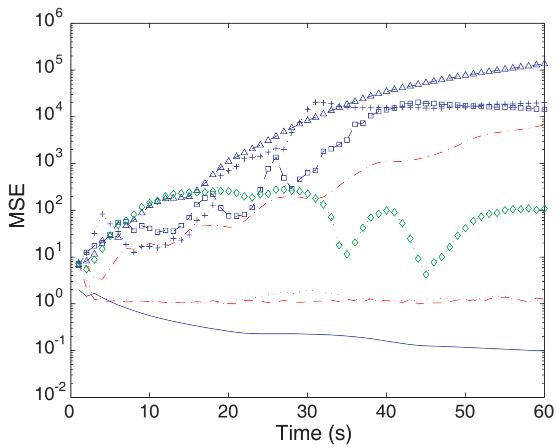

Figure 2. Mean square error comparison between Approach 1, 1-PNN and 3-PNN methods with process noise (— PCRLB; - · - PF of Approach 1; −− PF-EKF of Approach 1; ··· PF-UKF of Approach 1; △ PF of 1-PNN; □ PF-EKF of 1-PNN; + PF-UKF of 1-PNN; ⋄ PF-UKF of 3-PNN).

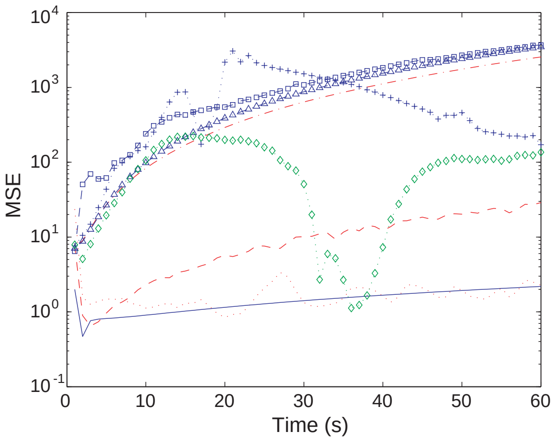

Figure 3. Mean square error comparison between Approach 2, 1-PNN 3-PNN methods without process noise (— PCRLB; - · - PF of Approach 2; −− PF-EKF of Approach 2; ··· PF-UKF of Approach 2; △ PF of 1-PNN; □ PF-EKF of 1-PNN; + PF-UKF of 1-PNN; ◇ PF-UKF of 3-PNN).

that the results of the proposed PF-EKF and PF-UKF schemes and PCRLB are similar in the absence and presence of process noise. The difference in the accuracy of PF-EKF and PF-UKF is around 1 m.

Next we consider a huge WSN of $M = 1000$ sensors. In this case, it is inappropriate to use the enumeration search to choose sensors because the combination of taking 3 out of $M = 1000$ is 166167000, which means that Approach 1 is infeasible. Instead, we examine the performance of Approach 2 and a $50\,\mathrm{m} \times 50\,\mathrm{m}$ square is chosen as the fixed area in the search. The MSE results for zero and non-zero process noise are shown in Figures 4 and 5, respectively. It is observed that the PF-UKF of Approach 2 gives the best tracking performance which is comparable to the PCRLB. It is because many sensors have been selected to provide observations at each time in this dense sensor network. However, the PF-EKF has more than 10 m difference in estimation accuracy. As we can see that PCRLB has fast drop at first due to the random initialization.

5.2. Evaluation of Approaches with Sensing Range Constraint

With sensing range constraint, we now evaluate the performance of Approaches 3 and 4 with $M = 1000$ sensors, and the results of zero and non-zero process noise, are plotted in Figures 6 and 7, respectively.

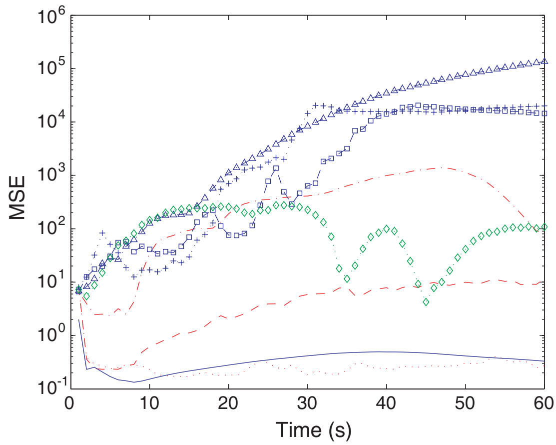

Figure 4. Mean square error comparison between Approach 2, 1-PNN and 3-PNN methods with process noise (— PCRLB; - · - PF of Approach 2; −− PF-EKF of Approach 2; ··· PF-UKF of Approach 2; △ PF of 1-PNN; □ PF-EKF of 1-PNN; + PF-UKF of PNN; ⋄ PF-UKF of 3-PNN).

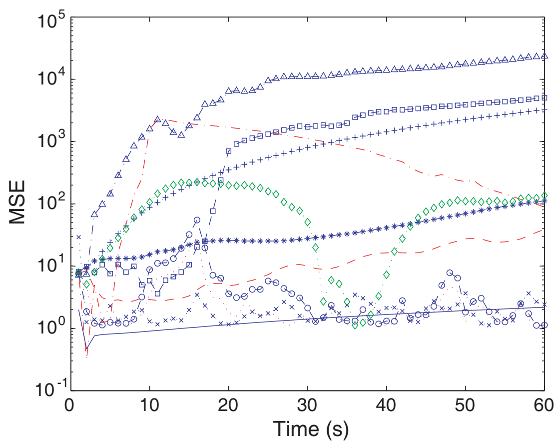

Figure 5. Mean square error comparison between Approaches 3, 4 and 1-PNN and 3-PNN methods without process noise (— PCRLB; ⋆ PF of Approach 3; ∘ PF-EKF of Approach 3; × PF-UKF of Approach 3; - · - PF of Approach 4; −− PF-EKF of Approach 4; ··· PF-UKF of Approach 4; △ PF of 1-PNN; □ PF-EKF of 1-PNN; + PF-UKF of 1-PNN; ⋄ PF-UKF of 3-PNN).

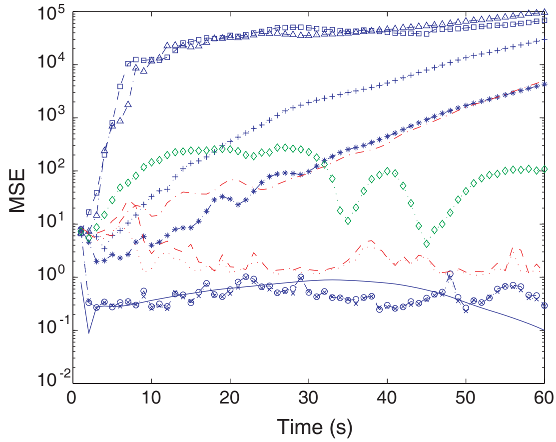

Figure 6. Mean square error comparison between Approaches 3, 4, 1-PNN and methods with process noise (— PCRLB; ⋆ PF of Approach 3; ○ PF-EKF of Approach 3; × PF-UKF of Approach 3; - · - PF of Approach 4; −− PF-EKF of Approach 4; ··· PF-UKF of Approach 4; △ PF of 1-PNN; □ PF-EKF of 1-PNN; + PF-UKF of 1-PNN; ⋄ PF-UKF of 3-PNN).

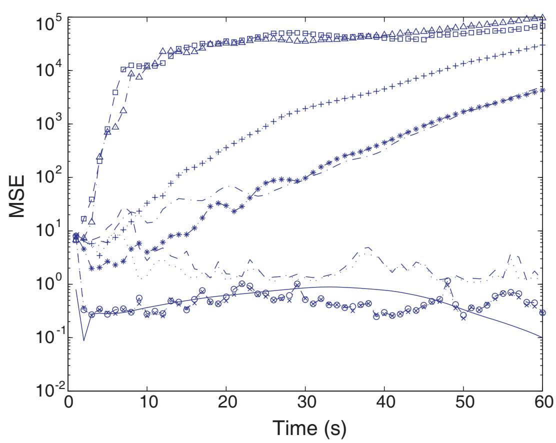

Figure 7. Mean square error comparison between Approaches 3-4 and PNN method with process noise (— PCRLB; ⋆ PF of Approach 3; ○ PF-EKF of Approach 3; × PF-UKF of Approach 3; - · - PF of Approach 4; −− PF-EKF of Approach 4; ··· PF-UKF of Approach 4; △ PF of PNN; □ PF-EKF of PNN; + PF-UKF of PNN).

The maximum communication range $r = 30\,\mathrm{m}$ is chosen. We see that the performance of the PF-EKF and PF-UKF of Approach 3 is the best among other trackers and attains the PCRLB. Since only $M_t = 3$ sensors are selected in Approach 4, the performance is not very good compared with using all sensors in the circle governed by r. In this test, the PF-EKF of Approach 3 is the recommended tracker as it provides the best performance with relatively smaller complexity.

6. CONCLUSIONS

In this paper, we have studied the sensor selection problem for target tracking in a wireless sensor network (WSN). Utilizing the posterior Cramer-Rao lower bound (PCRLB) without process noise, we have proposed four approaches to solve the sensor selection problem. Three particle filter (PF) schemes, namely, bootstrap, extended Kalman filter (EKF) and unscented Kalman filter (UKF), for target tracking are suggested. Without sensing range constraint, the PF-UKF of Approach 2 is the best tracker in a dense WSN. With sensing range constraint, the PF-EKF of Approach 3 is recommended as it provides the best performance with relatively smaller complexity.

ACKNOWLEDGMENT

The work described in this paper was supported by a grant from the Research Grants Council of the Hong Kong Special Administrative Region, China [Project No. CityU 122307].

REFERENCES

1. Patwari, N., J. N. Ash, S. Kyperountas, A. O. Hero III, R. L. Moses, and N. S. Correal, "Locating the nodes — Cooperative localization in wireless sensor networks," *IEEE Signal Processing Magazine*, Vol. 22, No. 4, 54–69, Jul. 2005.
2. Gezici, S., Z. Tian, G. B. Giannakis, H. Kobayashi, A. F. Molisch, H. V. Poor, and Z. Sahinoglu, "Localization via ultra-wideband radios: A look at positioning aspects for future sensor networks," *IEEE Signal Processing Magazine*, Vol. 22, No. 4, 70–84, Jul. 2005.
3. Zhao, F., J. Shin, and J. Reich, "Information-driven dynamic sensor collaboration," *IEEE Signal Processing Magazine*, Vol. 19, No. 2, 61–72, May 2002.
4. Guo, D. and X. Wang, "Dynamic sensor collaboration via

sequential Monte Carlo," *IEEE Journal on Selected Areas in Communications*, Vol. 22, No. 6, 1037–1047, Aug. 2004.

5. Isler, V. and R. Bajcsy, "The sensor selection problem for bounded uncertainty sensing models," *IEEE Trans. Automation Science and Engineering*, Vol. 3, No. 4, 372–380, Oct. 2006.
6. Tharmarasa, R., T. Kirubarajan, and M. L. Hernandez, "Large-scale optimal sensor array management for multitarget tracking," *IEEE Trans. Systems, Man, and Cybernetics — Part C: Applications and Reviews*, Vol. 37, No. 5, 803–814, Sep. 2007.
7. Chhetri, A. S., D. Morrell, and A. Papandreou-Suppappola, "The use of particle filtering with the unscented transform to schedule sensors," *Proc. ICASSP-04*, Vol. 2, 301–304, Montreal, QC, Canada, May 2004.
8. Thatte, G. and U. Mitra, "Sensor selection and power allocation for distributed estimation in sensor networks: Beyond the star topology," *IEEE Trans. Signal Processing*, Vol. 56, No. 7, 2649–2661, Jul. 2008.
9. Ristic, B., A. Arulampalam, and N. Gordon, *Beyond the Kalman Filter-particle Filters for Tracking Applications*, Artech House, Boston, 2004.
10. Vander Merwe, R., A. Doucet, N. de Freitas, and E. Wan, "The unscented particle filter," *Advances in Neural Information Processing Systems*, Vol. 13, MIT Press, Dec. 2000.
11. Arulampalam, M. S., S. Maskell, N. Gordon, and T. Clapp, "A tutorial on particle filters for online nonlinear/non-Gaussian Bayesian tracking," *IEEE Trans. Signal Processing*, Vol. 50, No. 2, 174–188, Feb. 2002.
12. Hue, C., J. Cadre, and P. Perez, "Sequential Monte Carlo methods for multiple target tracking and data fusion," *IEEE Trans. Signal Processing*, Vol. 50, No. 2, 309–325, Feb. 2002.
13. Bergman, N., *Recursive Bayesian Estimation: Navigation and Tracking Applications*, Ph.D. Thesis, Linkoping University, Sweden, 1999.
14. Tichavsky, P., C. H. Muravchik, and A. Nehorai, "Posterior Cramer-Rao bounds for discrete-time nonlinear filtering," *IEEE Trans. Signal Processing*, Vol. 46, No. 5, 1386–1396, May 1998.
15. Robert, C. P. and G. Casella, *Monte Carlo Statistical Methods*, Springer, New York, 1999.
16. Chen, J. F., Z. G. Shi, S. H. Hong, and K. S. Chen, "Grey prediction based particle filter for maneuvering target tracking," *Progress In Electromagnetics Research*, PIER 93, 237–254, 2009.